Long-lived coupled peeling ballooning modes preceding ELMs on JET

Identification of coupled peeling ballooning modes in JET

C. Perez von Thun,[1, 2, *] L. Frassinetti,[3] L. Horvath,[4] S. Saarelma,[5] L. Meneses,[6] E. de la Luna,[7] M. Beurskens,[8] J. Boom,[9] J. Flanagan,[5] C.F. Maggi,[5] S.J.P. Pamela,[5] E.R. Solano,[7] and JET Contributors[†]

[1] *Forschungszentrum Jülich GmbH, Institut für Energie- und Klimaforschung - Plasmaphysik, 52425 Jülich, Germany.*
[2] *EUROfusion PMU, Culham Science Centre, Abingdon, OX14 3DB, United Kingdom.*
[3] *Department of Fusion Plasma Physics, Royal Institute of Technology KTH, Stockholm, Sweden.*
[4] *York Plasma Institute, University of York, Heslington, York, YO10 5DD, UK*
[5] *Culham Centre for Fusion Energy, Abingdon, OX14 3DB, UK.*
[6] *Instituto de Plasmas e Fusão Nuclear, IST, Universidade de Lisboa, 1049-001 Lisboa, Portugal.*
[7] *Laboratorio Nacional de Fusion, CIEMAT, E-28040, Madrid, Spain.*
[8] *Max-Planck-Institut für Plasmaphysik, Wendelsteinstr. 1, D-17491 Greifswald, Germany.*
[9] *Max-Planck-Institut für Plasmaphysik, Boltzmannstr. 2, D-85748 Garching, Germany.*

(Dated: March 2, 2018)

Edge localised oscillations with toroidal mode number $n \leq 16$ regularly preceding type-I Edge Localised Mode (ELM) crashes at sufficiently low pedestal collisionality ($\nu^*_{ee,ped} \lesssim 0.25$) on JET are identified as coupled peeling ballooning modes. This extends and generalises to higher mode numbers the work by [Huysmans et al Nucl. Fusion 38 (1998) 179], which identified the lowest n modes (also termed 'outer modes') as external kinks. The identification of these modes opens up a new avenue to test existing ELM models. Possibilities to reconcile the relatively long lifetime of these modes (typically one to few tens of ms) with widely supported physics models that predict the ELM to be triggered by peeling ballooning modes are discussed.

The edge region of high confinement ('H-mode') tokamak plasmas has a strong influence on the fusion performance of the tokamak as a whole. A narrow boundary layer with reduced transport ('pedestal') develops with steep density and temperature gradients that can drive a variety of macroscopic instabilities. The increase in plasma stored energy is limited by quasi-periodic bursts called Edge Localised Modes (ELMs) [1], which lead to a transient collapse of the pedestal. Understanding these modes is imperative for correctly predicting fusion performance and controlling ELMs in ITER.

Coupling of the (pressure driven) edge ballooning mode to the (current driven) external kink (or 'peeling') mode was first theoretically predicted by Connor et al [2]. The excitation of these coupled peeling ballooning (PB) modes was put forward in what has become the most widely accepted model to explain the occurrence of ELMs, the PB model.

The validity of the PB model has been investigated experimentally mainly with detailed pedestal profile measurements, and theoretically with help of MHD stability codes. Also, this model is used as a constraint in the predictive pedestal model EPED [3, 4], which has been used to predict the limiting pressure pedestal height and width for several present tokamaks, with overall good success [4, 5]. On JET, the EPED model works quite well at low gas fuelling, but not so well at high gas rates [6–9].

However, the experimental identification of the PB modes themselves has so far been outstanding. The work presented here closes this gap by systematically comparing the experimental MHD fluctuation measurements of the pedestal, specifically on JET, for a wide operational range, and comparing the results with stability modelling predictions.

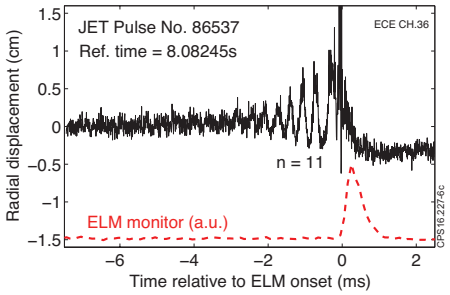

FIG. 1. Example of $n = 11$ oscillations anticipating an ELM, measured with ECE in the steep region of the pedestal. Be-II light emitted in divertor is used as ELM monitor. Typically, the radial displacement associated with these modes as seen by both reflectometry and ECE is of order few mm up to 1cm. For comparison, the pressure pedestal width on JET is of order 2cm.

Empirically, in some discharges on JET type I ELM crashes are regularly preceded by a class of low frequency ($\lesssim$20kHz) oscillations [10], as in figure 1. Identification of the nature of these modes was so far largely prevented by the limited edge profile information available. Making use of improved edge diagnostics, a database has now been compiled for 460 deuterium discharges, including discharges run with either a CFC-based or a Be/W-based (ITER-like) first wall, with and without oscillations. The database combines electron density (n_e) and temperature (T_e) profiles from high resolution Thomson Scattering (HRTS) with fast fluctuation data from Mirnov coils and electron cyclotron emission (ECE). To obtain representative profiles, for each discharge HRTS profile data

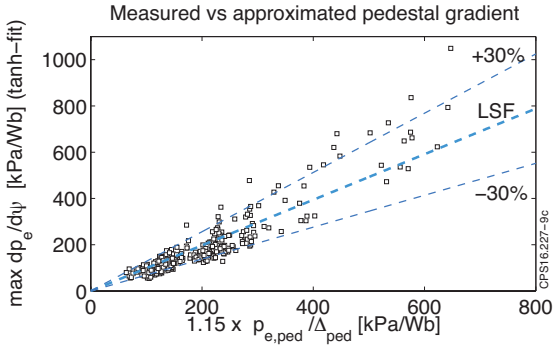

FIG. 2. Comparison of maximum pedestal electron pressure gradient extracted from (pre-ELM) tanh-fitted profiles with a KBM-based approximation formula that relies on pedestal top measurements only.

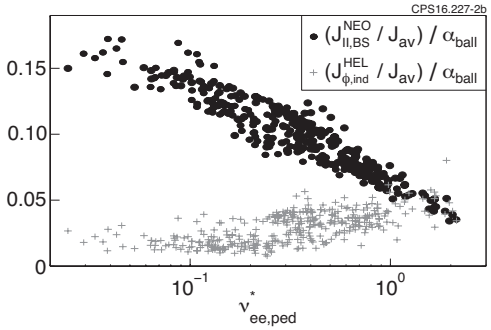

FIG. 3. Normalised maximum flux surface averaged bootstrap current density $<J_{||,\mathrm{BS}}B>/B_0$ (for brevity, $J^{\mathrm{NEO}}_{||,\mathrm{BS}}$) computed by the first principles kinetic code NEO [16, 17] for a subset of the database, as a function of pedestal top collisionality. Also shown is the toroidal Ohmic current density $J^{\mathrm{HEL}}_{\phi,\mathrm{ind}}$ with same normalisation, computed by the HELENA code.

during the last 30% of an ELM cycle has been averaged over several ELM cycles and fitted with a modified hyperbolic tangent [11, 12]. Due to instrument vignetting, for some (older) parts of the database only pedestal top values are available.

The analysis is done in terms of dimensionless, MHD relevant variables. For the pressure drive of ballooning modes, we have approximated the maximum normalised pressure gradient (ballooning alpha, α_{ball} [13]) across the pedestal as $\widehat{\alpha}_{\mathrm{ball}} = -2\mu_0 R p'_{\mathrm{KBM}} q^2_{95}/B^2_0$, with $p'_{\mathrm{KBM}} = c(1+\gamma_i)n_{e,ped}T_{e,ped}/\Delta_{\mathrm{KBM}}$. Here, R is the major radius, q_{95} is the safety factor at 95% of normalised flux, B_0 is the magnetic field on axis, $\gamma_i(Z_{\mathrm{eff}}) < 1$ accounts for the main ion dilution by impurities, the subscript "ped" denotes the pedestal top value, $\Delta_{\mathrm{KBM}} = 0.076\beta^{1/2}_{\mathrm{pol,ped}}$ is a kinetic ballooning mode (KBM) based scaling for the pedestal width [4] and $c = 1.15$ is a constant empirical factor. This assumes $T_{i,ped}$=$T_{e,ped}$, which is a good approximation near the plasma boundary. Thus, the maximum pedestal pressure gradient is replaced with an easier to measure "top/width" based approximation. Dedicated scans on JET have revealed cases where the pedestal width is not well described by a KBM scaling [8, 9, 14]. Despite that, comparing this approximation with the fitted profile gradients of 350 discharges yields only a moderate standard deviation of 24% (figure 2).

As a proxy for the normalised current drive $J_{||}/J_{\mathrm{av}}$ for the peeling modes (with J_{av} the average current density across the plasma), the neoclassical pedestal top collisionality ($\nu^*_{\mathrm{ee,ped}}$) can be used. This is because the boostrap current [15], which typically dominates in the edge region, is roughly proportional to the pressure gradient, but is reduced by collisions. Hence, as the collisionality is reduced, more current is produced at a given pressure gradient. Figure 3 demonstrates this explicitly for our case and quantifies by how much the bootstrap current varies across the database (factor 4-5 within this normalisation, which is significant). Figure 3 also includes the toroidal Ohmic current contribution $J_{\phi,\mathrm{ind}}$ at the radial location of the maximum bootstrap current, equally normalised, from a separate computation with the HELENA code [18]. It has some tendency to increase at high collisionality, but overall the Ohmic contribution has a more flat dependence on $\nu^*_{\mathrm{ee,ped}}$. So, in first approximation we can consider it introduces simply a constant offset and the trend for the overall edge current to decrease with collisionality remains valid.

Figure 4 plots the full database in $\widehat{\alpha}_{\mathrm{ball}}$-$\nu^*_{\mathrm{ee,ped}}$ space, distinguishing between low (LT) and high (HT) triangularity of the poloidal plasma cross section (which is well known to be a key player for ballooning stability, as shown in the adjacent cartoon) and between cases with and without modes. At lower edge current (high $\nu^*_{\mathrm{ee,ped}}$), LT and HT datapoints run approximately parallel (same α increase for given reduction in $\nu^*_{\mathrm{ee,ped}}$, i.e. increase in $J_{||}/J_{\mathrm{av}}$). This is the domain of the "pure" ballooning mode (no peeling component). At low $\nu^*_{ee,ped}$, both groups of datapoints diverge, such that for a given increase in edge current density the α increase is more pronounced at high shaping. The transition between the two regimes marks the region highlighted in the neighbouring cartoon, and is found to happen in JET at $\nu^*_{\mathrm{ee,ped}}(crit) \sim$ 0.15-0.3. Crucially, mode activity (full symbols) is routinely observed only for $\nu^*_{\mathrm{ee,ped}}$<$\nu^*_{\mathrm{ee,ped}}(crit)$, while for $\nu^*_{\mathrm{ee,ped}}$>$\nu^*_{\mathrm{ee,ped}}(crit)$ (the pure ballooning region) mode activity is generally absent (open symbols). Near the transition region, $\nu^*_{\mathrm{ee,ped}}$~$\nu^*_{\mathrm{ee,ped}}(crit)$, either case can be found. Not using a "top/width" approximation but plotting directly in $J_{||,\mathrm{BS}}/J_{\mathrm{av}}$ and HELENA α_{ball} coordinates (not shown here) for a reduced subset of the database confirms this trend.

The above interpretation is also confirmed by comparison of individual discharges with stability calculations by the finite-n MHD code MISHKA-1 [19], using analytical edge current approximations close to the NEO prediction

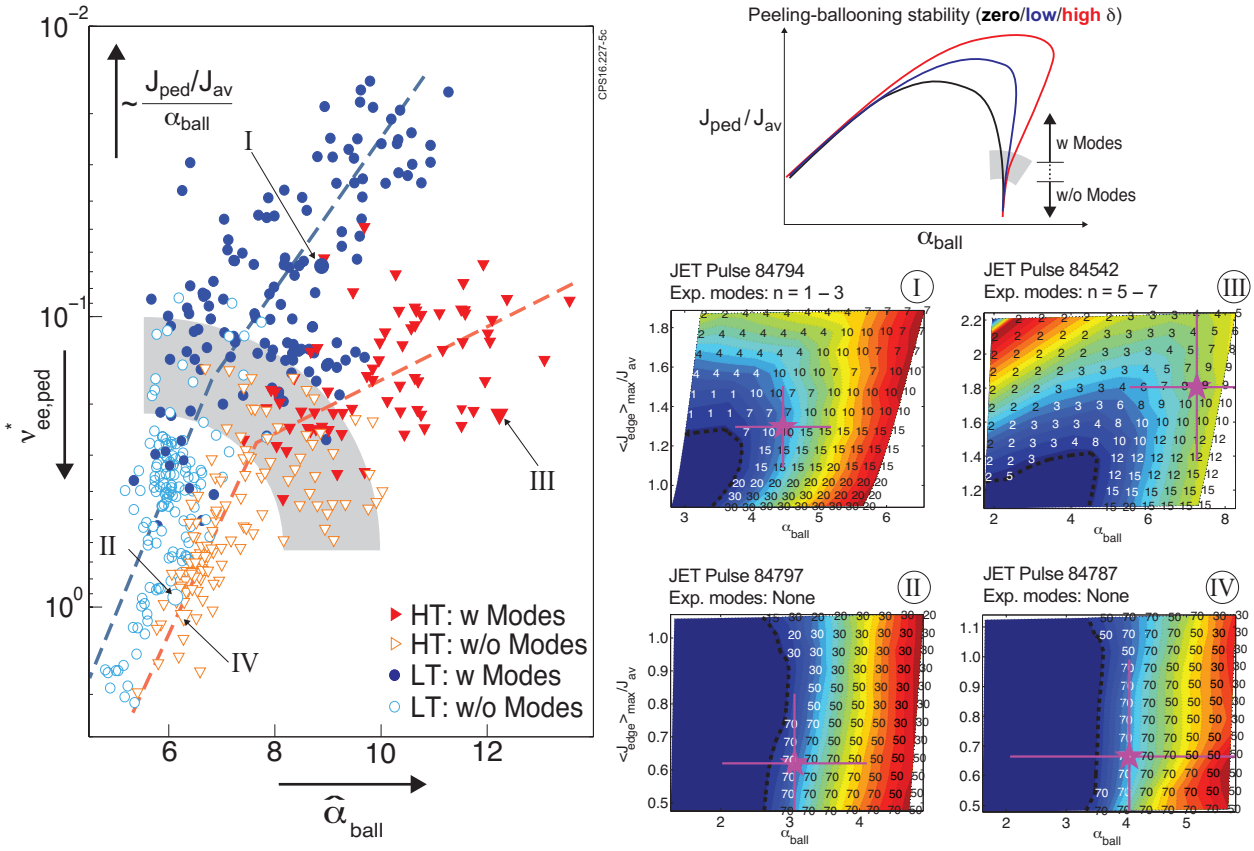

FIG. 4. (Left:) Existence domain of cases with (full symbols) and without modes (open symbols), in $\widehat{\alpha}_{\rm ball}$-$\nu^*_{\rm ee,ped}$ coordinates, distinguishing high ($0.33 < \delta < 0.47$) and low ($0.19 < \delta < 0.31$) plasma triangularity. Notice in this plot the collisionality (y-axis) direction is inverted, increasing from top to bottom. The lines and shaded transition area are to guide the eye, with colours matching the adjacent PB stability cartoon (top right). MISHKA stability calculations for four discharges (see labels I-IV on left) are shown underneath. Here, the overlaid numbers indicate the most unstable n numbers (font colour choice for easier read) predicted in stability space, background shade denotes growth rate (increases from blue to red) and the operational point with estimated uncertainty is shown in magenta. For comparison, information on the experimentally observed modes for each of the four cases is included in the titles. It should be noted that MISHKA uses a different formula for $\alpha_{\rm ball}$ (we use HELENA definition), hence $\alpha_{\rm ball}$ absolute values do not coincide with left plot. In the MISHKA plots, the edge current includes the inductive contribution, and the bootstrap contribution was computed using analytical approximation formulas which agree with NEO to within 20%.

(Sauter[20, 21] or Hager[22], depending on the collisionality). Four cases along both extremes are shown in subfigures I-IV. MISHKA predicts the open symbols are in or near the domain susceptible to high-n = 30-70 pure ballooning instabilities, whereas the full symbols are near or inside the stability nose where intermediate $n \leq 15$ PB modes are predicted to be most unstable. Also, the experimental data in figure 4 shows little indication of a decrease in $\alpha_{\rm ball}$ even at the highest edge current densities, i.e. the pedestal remains limited by pressure, not current, across the entire database. This is in agreement with MISHKA, which also shows the pre-ELM profiles to sit on or nearer to the pressure-bound side of the stability triangle.

The toroidal mode number n of oscillations has been reconstructed using an array of toroidally distributed magnetic pick-up coils. The statistical distribution of the experimentally observed n numbers from 300 discharges is depicted in figure 5 in stability coordinates. The full coloured symbols mark the average coordinates of the "cloud" of data points with same n and the bars show the extent of their existence domain, i.e. the standard deviation of the "cloud" (not the measurement uncertainty). The limited size of the bars is very remarkable considering the heterogeneity of the database, which covers a large range of plasma current (I_p =1.3-4.5 MA), toroidal field (B_0 =1.7-3.6T), edge safety factor (q_{95} =2.6-4.8), plasma shape (δ = 0.19-0.47), heating (P_{aux} =4-27MW) and fuelling rates, and demonstrates these coordinates are succesfully capturing the physics of these modes. The overlap between domains is real as often several modes with different n co-exist in the plasma [10]. Crucially, the

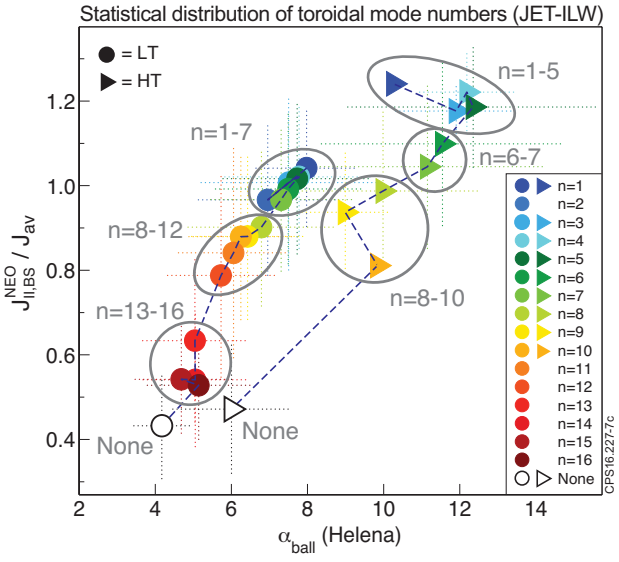

FIG. 5. Occurrence domains of experimental mode numbers for a subset of the database (JET-ILW) with full profile information from HRTS, mapped into $J_{||,\mathrm{BS}}/J_{\mathrm{av}}$ (computed by NEO) and α_{ball} (computed by HELENA) coordinates. The dashed lines connects subsequent mode numbers at low (circles) and high (triangles) triangularity. Mode numbers are almost perfectly ordered moving from high to low n with increasing bootstrap current.

mode number domains are almost strictly sorted statistically from high n at low $J_{||,\mathrm{BS}}/J_{\mathrm{av}}$ and low α_{ball} to low n at high $J_{||,\mathrm{BS}}/J_{\mathrm{av}}$ and high α_{ball}. This is in agreement with PB mode theory: increasing edge current density is stabilising for ballooning modes (high n) and destabilising for peeling modes (lower n). The "no-mode" domain is at lower $J_{||,\mathrm{BS}}/J_{\mathrm{av}}$ and α_{ball}. As was mentioned, this is the domain where high n = 30-70 pure ballooning modes were predicted by MISHKA. Such mode numbers could no longer be resolved with our toroidal coil array (maximum currently resolvable n is 25). A further (possibly lower) detection limit is imposed through radial damping of magnetic perturbations, which increases exponentially with poloidal mode number m.

Going a step further, for attempting a 1:1 comparison of the experimentally observed toroidal mode numbers with the most unstable n values predicted by MISHKA a good understanding of the uncertainties involved is critical. To this end, we selected a set of 18 discharges scanning from low to high collisionality at low and high shaping whose HRTS data was subjected to an even more meticulous analysis for best possible profile accuracy and statistical error information. This set includes the four examples shown in figure 4. Assuming that NEO yields a good approximation of the actual edge current density in the plasma, and that the overall error is dominated by the profile gradient determination, we find that in 16 out of 18 cases MISHKA is consistent with the experiment while in 2 cases MISHKA predicts a higher n. E.g., a case with good agreement is subfigure III, where the experimental mode numbers 5-7 also feature among the most unstable ones predicted by MISHKA within the J-α uncertainty, whereas subfigure I shows a case with not so good agreement (here the observed n = 1-3 modes are seen to be most unstable only just outside the uncertainty area). It is worth noting that if we just consider n values at the nominal operational point (star-symbol), we find that there is a general tendency for MISHKA to give a higher estimate than seen in experiment. Also, it has been generally noticed in the past that for JET plasmas MISHKA almost never predicts operational points accessing the lowest $n < 3$ (kink) domain. One possible explanation for these two observations could be edge velocity shear, which has not been included in the MISHKA calculations and is known to be destabilising for low n kink modes [23].

Summarising, the pre-ELM oscillations on JET are edge localised oscillations encountered only at sufficient edge current density; are encountered in the J-α domain expected for PB modes but not pure ballooning modes; the balance of J and α for a given shape determines their mode number with n as expected from PB mode theory, with n clearly observed statistically to increase with decreasing J; and can reach radial displacement amplitudes of a significant fraction of the pedestal width. Together with earlier findings: (a) they rotate in the ion (not electron) diamagnetic direction and the radial mode structure of these oscillations has kink (not tearing) parity [10], and (b) the lowest n modes have been identified as external kink modes through analysis of 2D Soft X-Ray data [24], it is justified to identify the pre-ELM oscillations as coupled PB ballooning modes with gradual transition into pure peeling modes with decreasing mode number. Also, magnetics see increasing in-board/outboard (ballooning) amplitude asymmetry with increasing mode number which are at least consistent with this identification, but here radial damping in-/out-asymmetries also need to be considered [10].

The identification of these modes opens up a new avenue to test existing ELM models. It should be emphasized that it has not yet been demonstrated that these modes trigger the ELM. While the pre-ELM oscillations are often seen to grow into an ELM, they can also saturate in amplitude and last for several tens of ms before an ELM crash is triggered [10]. One possibility is that the strong velocity shear that is known to exist in the pedestal region delays the ELM onset, by trapping the mode filaments inside the separatrix [25]. Rotational shear has also been proposed to explain the saturation of Edge Harmonic Oscillations [26] in Quiescent H-mode plasma regime [27], which are believed to be external kink modes. Another possibility is that only pure ballooning modes have explosive non-linear growth leading to the ELM [28, 29], while peeling modes (on their own or

coupled to ballooning modes) are inherently more benign and non-linearly saturate. But they would still facilitate ELMs if ballooning modes emerge out of the oscillating mode as a secondary instability. This picture is indeed qualitatively consistent with ECE imaging observations of ELMs on KSTAR, reporting narrow fingerlike perturbations growing out of a saturated state [30]. It would also explain why ELMs are still triggered on JET whilst deeply in the high-n ballooning corner of stability and in the absence of pre-ELM oscillations. This hypothesis could be tested further through non-linear MHD simulations.

This work has been carried out within the framework of the EUROfusion Consortium and has received funding from the Euratom research and training programme 2014-2018 under grant agreement No 633053. The views and opinions expressed herein do not necessarily reflect those of the European Commission.

* Email for correspondence: christian.perezvonthun@eurofusion.org

† See the author list of "X. Litaudon et al 2017 Nucl. Fusion 57 102001".

[1] H. Zohm, Plasma Physics and Controlled Fusion **38**, 105 (1996).

[2] J. W. Connor, R. J. Hastie, H. R. Wilson, and R. L. Miller, Physics of Plasmas **5**, 2687 (1998).

[3] P. B. Snyder, R. J. Groebner, A. W. Leonard, T. H. Osborne, and H. R. Wilson, Physics of Plasmas **16**, 056118 (2009), http://dx.doi.org/10.1063/1.3122146.

[4] P. B. Snyder, R. J. Groebner, J. W. Hughes, T. H. Osborne, M. Beurskens, A. W. Leonard, H. R. Wilson, and X. Q. Xu, Nuclear Fusion **51**, 103016 (2011).

[5] R. J. Groebner *et al.*, Nuclear Fusion **53**, 093024 (2013).

[6] M. N. A. Beurskens, L. Frassinetti, C. Challis, C. Giroud, S. Saarelma, B. Alper, C. Angioni, P. Bilkova, C. Bourdelle, S. Brezinsek, P. Buratti, G. Calabro, T. Eich, J. Flanagan, E. Giovannozzi, M. Groth, J. Hobirk, E. Joffrin, M. J. Leyland, P. Lomas, E. de la Luna, M. Kempenaars, G. Maddison, C. Maggi, P. Mantica, M. Maslov, G. Matthews, M.-L. Mayoral, R. Neu, I. Nunes, T. Osborne, F. Rimini, R. Scannell, E. R. Solano, P. Snyder, I. Voitsekhovitch, P. de Vries, and J.-E. Contributors, Nuclear Fusion **54**, 043001 (2014).

[7] S. Saarelma, A. Jrvinen, M. Beurskens, C. Challis, L. Frassinetti, C. Giroud, M. Groth, M. Leyland, C. Maggi, J. Simpson, and J. Contributors, Physics of Plasmas **22**, 056115 (2015), http://dx.doi.org/10.1063/1.4921413.

[8] C. F. Maggi, S. Saarelma, F. J. Casson, C. Challis, E. de la Luna, L. Frassinetti, C. Giroud, E. Joffrin, J. Simpson, M. Beurskens, I. Chapman, J. Hobirk, M. Leyland, P. Lomas, C. Lowry, I. Nunes, F. Rimini, A. Sips, and H. Urano, Nuclear Fusion **55**, 113031 (2015).

[9] M. J. Leyland, M. N. A. Beurskens, L. Frassinetti, C. Giroud, S. Saarelma, P. B. Snyder, J. Flanagan, S. Jachmich, M. Kempenaars, P. Lomas, G. Maddison, R. Neu, I. Nunes, and K. J. Gibson, Nuclear Fusion **55**, 013019 (2015).

[10] C. P. Perez, H. R. Koslowski, G. T. A. Huysmans, T. C. Hender, P. Smeulders, B. Alper, E. de la Luna, R. J. Hastie, L. Meneses, M. F. F. Nave, V. Parail, M. Zerbini, and J.-E. Contributors, Nuclear Fusion **44**, 609 (2004).

[11] R. J. Groebner, D. R. Baker, K. H. Burrell, T. N. Carlstrom, J. R. Ferron, P. Gohil, L. L. Lao, T. H. Osborne, D. M. Thomas, W. P. West, J. A. Boedo, R. A. Moyer, G. R. McKee, R. D. Deranian, E. J. Doyle, C. L. Rettig, T. L. Rhodes, and J. C. Rost, Nuclear Fusion **41**, 1789 (2001).

[12] L. Frassinetti, M. N. A. Beurskens, R. Scannell, T. H. Osborne, J. Flanagan, M. Kempenaars, M. Maslov, R. Pasqualotto, and M. Walsh, Review of Scientific Instruments **83**, 013506 (2012), http://dx.doi.org/10.1063/1.3673467.

[13] J. W. Connor, R. J. Hastie, and J. B. Taylor, Phys. Rev. Lett. **40**, 396 (1978).

[14] L. Frassinetti, M. N. A. Beurskens, S. Saarelma, J. E. Boom, E. Delabie, J. Flanagan, M. Kempenaars, C. Giroud, P. Lomas, L. Meneses, C. S. Maggi, S. Menmuir, I. Nunes, F. Rimini, E. Stefanikova, H. Urano, G. Verdoolaege, and J. Contributors, Nuclear Fusion **57**, 016012 (2017).

[15] F. L. Hinton and R. D. Hazeltine, Rev. Mod. Phys. **48**, 239 (1976).

[16] E. A. Belli and J. Candy, Plasma Physics and Controlled Fusion **50**, 095010 (2008).

[17] E. A. Belli and J. Candy, Plasma Physics and Controlled Fusion **54**, 015015 (2012).

[18] G. T. A. Huysmans, J. P. Goedbloed, and W. Kerner, in *Proc. CP90 Europhys. Conf. on Comput. Phys.*, Amsterdam, The Netherlands (10-13 September 1990), edited by A. Tenner (Singapore: World Scientific, 1991) pp. 371–376.

[19] A. B. Mikhailovskii *et al.*, Plasma Phys. Rep. **23**, 844 (1997).

[20] O. Sauter, C. Angioni, and Y. R. Lin-Liu, Physics of Plasmas **6**, 2834 (1999).

[21] O. Sauter, C. Angioni, and Y. R. Lin-Liu, Physics of Plasmas **9**, 5140 (2002), https://doi.org/10.1063/1.1517052.

[22] R. Hager and C. S. Chang, Physics of Plasmas **23**, 042503 (2016), http://dx.doi.org/10.1063/1.4945615.

[23] P. B. Snyder, K. H. Burrell, H. R. Wilson, M. S. Chu, M. E. Fenstermacher, A. W. Leonard, R. A. Moyer, T. H. Osborne, M. Umansky, W. P. West, and X. Q. Xu, Nuclear Fusion **47**, 961 (2007).

[24] G. T. A. Huysmans, T. C. Hender, and B. Alper, Nuclear Fusion **38**, 179 (1998).

[25] A. Kirk, D. Dunai, M. Dunne, G. Huijsmans, S. Pamela, M. Becoulet, J. R. Harrison, J. Hillesheim, C. Roach, and S. Saarelma, Nuclear Fusion **54**, 114012 (2014).

[26] X. Chen, K. H. Burrell, N. M. Ferraro, T. H. Osborne, M. E. Austin, A. M. Garofalo, R. J. Groebner, G. J. Kramer, N. C. L. Jr, G. R. McKee, C. M. Muscatello, R. Nazikian, X. Ren, P. B. Snyder, W. M. Solomon, B. J. Tobias, and Z. Yan, Nuclear Fusion **56**, 076011 (2016).

[27] A. M. Garofalo, K. H. Burrell, D. Eldon, B. A. Grierson, J. M. Hanson, C. Holland, G. T. A. Huijsmans, F. Liu, A. Loarte, O. Meneghini, T. H. Osborne, C. Paz-Soldan, S. P. Smith, P. B. Snyder, W. M. Solomon, A. D. Turnbull, and L. Zeng, Physics of Plasmas **22**, 056116 (2015),

http://aip.scitation.org/doi/pdf/10.1063/1.4921406.
[28] H. R. Wilson and S. C. Cowley, Phys. Rev. Lett. **92**, 175006 (2004).
[29] C. J. Ham, S. C. Cowley, G. Brochard, and H. R. Wilson, Phys. Rev. Lett. **116**, 235001 (2016).
[30] G. S. Yun, W. Lee, M. J. Choi, J. Lee, H. K. Park, B. Tobias, C. W. Domier, N. C. Luhmann, A. J. H. Donné, and J. H. Lee (KSTAR Team), Phys. Rev. Lett. **107**, 045004 (2011).